Comparison of K-E Turbulence Model Wall Functions Applied on a T-Junction Channel Flow

G. C. C. Fiuza[1], A. L. T. Rezende[2]

Mechanical and Materials Engineering Department, IME – Military Instituto of Engineering, RJ, Brazil

Abstract**—***The flow acting in a T-junction channel is present in several industrial applications, such as air conditioning systems, water cooling circuits, gas exhaust systems and others. In order to numerically simulate this case, the Average Reynolds Navier-Stokes (RANS) equation is used for a two-dimensional stationary flow using the k-ε model together with wall functions such as standard wall function, Enhanced and Menter-Lechner wall treatments. The moment ratio used is M_R = 2 and the Reynolds number at the inlet of the flow parallel to the channel is Re = 15,000. The results were compared with the literature data using Large Scale Simulation (LES). The results obtained for k-ε model Enhanced and Menter-Lechner wall treatment were satisfactory and close to that found by the LES simulation, however, results obtained from k-ε model standard wall function presented large deviation to literature, mainly in the boundary layer and K production profiles. In general, the results presented small distortions for the profiles of turbulent kinetic energy production near walls, however, they illustrate in an analogous manner to the literature the production of turbulent kinetic energy K concentrated in the shear layers between flows. The main results analyzed in this paper are the length of the recirculation bubble, boundary layer profile, mean velocity magnitude and kinetic energy production k.*

Keywords**—Turbulence, RANS, k-ε, T-Junction, Channel, LES.**

I. INTRODUCTION

The main objective of the present work is the computational analysis of the geometry of a rectangular T-junction channel. In this situation, a flow parallel to the channel, called "parallel flow", enters the main channel and another flow transversal to the channel, called “jet flow”, enters the jet flow inlet. As the parallel flow approaches the inlet region of the jet stream, it bypasses the jet flow due to the high jet flow momentum. Since the parallel flow cannot penetrate the jet flow, it contours the jet flow as an obstacle. In addition, the jet flow cannot penetrate the parallel flow, curving until it becomes parallel to the parallel flow and the channel. Such changes of direction generate recirculation bubbles close to the inlet of the jet stream to the channel. This phenomenon, as illustrated in Fig. 1, has been extensively studied in the field of fluid dynamics and can be easily found in air conditioning, water cooling circuit in nuclear power plants, exhaust gas recirculation in internal combustion engines among other systems [1].

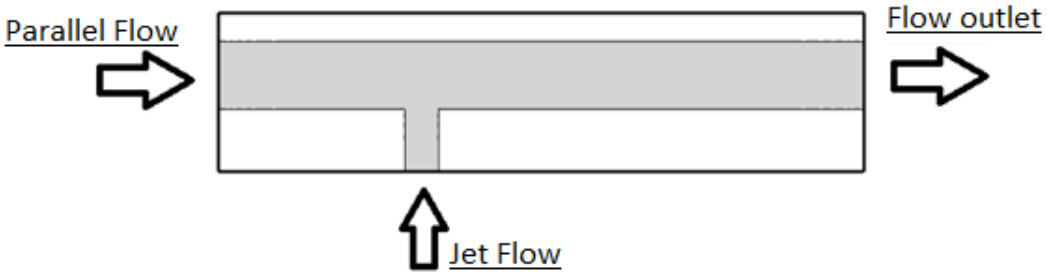

FIGURE 1: CHARACTERISTIC OF A FLOW IN A T-JUNCTION CHANNEL.

The simulations were performed based on the Reynolds Averaged Navier-Stokes (RANS) Equations with Reynolds number Re = 15,000 at the inlet of the parallel flow. The Reynolds number is defined as a function of the channel hydraulic diameter, kinematic viscosity and average flow velocity, given by (1):

$$Re = (U \times d_h)/\upsilon \tag{1}$$

where the hydraulic diameter for a rectangular channel is known according to (2):

$$d_h = (2 * H * L)/(H + L) \tag{2}$$

In order to compare the parallel flow (parallel to the channel) and jet flow (transversal to the channel), the fluid momentum ratio was used. This momentum ratio is defined as a function of the flow velocity, cross-sectional area of the channel and the density of each fluid given by (3):

$$M_R = \frac{(\rho U^2 A)_{Parallel\ \ Flow}}{(\rho U^2 A)_{Jet\ \ Flow}} \tag{3}$$

The performance of the turbulence model used for the case analysed in the present work was evaluated by comparison with the numerical results obtained by [1]. Georgiou and Papalexandris performed a numerical simulation with Re = 15.000 for the parallel flow inlet and used the Large Scale Simulation (LES) model with treatment in regions close to the wall for the analysis of a T-junction channel for flows with moment ratio of M_R= 2 and M_R= 0.5.Based on previous studies, this work presents numerical results of a T-junction channel geometry using the k-ε turbulence model in flows with moment ratio M_R= 2. The results obtained were compared with the analysis of [1].

II. MATHEMATICAL DESCRIPTION

The flow through a T-junction channel is governed by the application of the RANS Equations that describe the incompressible fluid movement. These equations are equations of conservation of momentum and continuity, being presented in (4):

$$\left(\frac{\partial u_i u_j}{\partial x_j}\right) = g_i - \frac{1}{\rho}\frac{\partial p}{\partial x_i} + \frac{\partial}{\partial x_j}\left(\upsilon \frac{\partial u_i}{\partial x_j}\right);\ \frac{\partial u_j}{\partial x_j} = 0 \tag{4}$$

The method of the average Reynolds equations is based on the decomposition of the instantaneous velocity value in the equation $u_i = \overline{u_i} + u_i'$,, where u_i represents the instantaneous velocity value, $\overline{u_i}$ the mean velocity vector and u_i' represents the velocity fluctuation vector [2]. Consequently, the mean momentum equation for non-transient and incompressible flows is given by (5):

$$\frac{\partial \overline{u_i}\overline{u_j}}{\partial x_j} = g_i - \frac{1}{\rho}\frac{\partial \bar{p}}{\partial x_i} + \frac{\partial}{\partial x_j}\left(\nu \frac{\partial \overline{u_i}}{\partial x_j} - \overline{u_i' u_j'}\right);\ \frac{\partial \overline{u_j}}{\partial x_j} = 0 \tag{5}$$

The term $\overline{u_i' u_j'}$ present in (5) is the Reynolds tensor and represents the influence of velocity fluctuations on the mean flow. However, (5) does not represent a closed system of equations, so it is necessary to determine the value of Reynolds turbulent tensor to close the system. For this, an analogy is made to Stokes's Law, based on the Boussinesq hypothesis, where the turbulent stresses are proportional to the mean velocity gradient of the flow. (6) represents the equation of the Reynolds tensor:

$$-\overline{u_i' u_j'} = \upsilon_t \left(\frac{\partial \overline{u_j}}{\partial x_j} + \frac{\partial \overline{u_j}}{\partial x_i}\right) - \frac{2}{3} k \delta_{ij}\ ;\ k = \frac{1}{2}\overline{u_i' u_i'} \tag{6}$$

The term υ_t is characterized as turbulent viscosity and is defined according to models of turbulence. There are several models of turbulence to find the term, but in this work, the k-ε model will be used.

2.1 k-ε Model

The standard k-ε model, developed by [3] and [4], is understood as a turbulence model of two conservation equations. Here two partial differential equations are solved, one for the turbulent kinetic energy k and the other for the dissipation of the turbulent kinetic energy per unit mass ε present respectively in (7) and (8).

$$\rho \frac{\partial k}{\partial t} + \rho \frac{\partial}{\partial x_j}\left(\overline{u_j} k\right) = \frac{\partial}{\partial x_j}\left[\left(\mu + \frac{\mu_t}{\sigma_k}\right)\frac{\partial k}{\partial x_j}\right] + P_k - Y_k \tag{7}$$

$$\rho \frac{\partial \varepsilon}{\partial t} + \rho \frac{\partial}{\partial x_j}\left(\overline{u_j} \varepsilon\right) = D_\varepsilon + P_\varepsilon - d_\varepsilon \tag{8}$$

where the terms P_k and Y_k are respectively the terms of production and destruction of turbulent kinetic energy k, and the terms D_ε, P_ε and d_ε are respectively the terms of diffusion, production and destruction of the specific rate of dissipation of turbulent kinetic energy per unit mass ε and the turbulent viscosity is given in (9) below:

$$\mu_t = \frac{C_\mu k^2}{\varepsilon} \tag{9}$$

C_μ is a constant with a value of 0.09, k is the turbulent kinetic energy and ε is the dissipation of turbulent kinetic energy per unit mass.Although the present model is widely used and obtains good results for simple flows with small pressure gradients, it has low precision in the vicinity of adverse pressure gradients [5].

2.2 Standard Wall Function

Law of the Wall are empirical relations used to connect the calculated quantities in the neighboring cells to the wall and the corresponding quantities in the wall. Experimentally three regions are verified in a turbulent boundary layer according to Fig. 2 below. The first layer located near the wall is called the viscous sub-layer. In this region of the flow the transport of momentum is carried out by means of molecular diffusive effects, resembling a laminar flow. In turn, the region of the logarithmic layer has as its characteristic the equivalence between the molecular and turbulent transport in the flow. Finally, the turbulent layer is fully dominated by the turbulent flow effects [6].

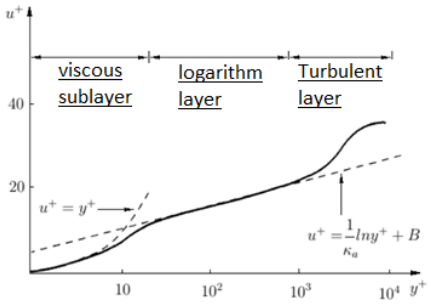

FIGURE 2: BOUNDARY LAYER PROFILE. [6]

The most common approach for near-wall velocity processing with respect to numerical simulations is performed by means of standard wall functions. By means of empirical formulations the flow is modeled in regions near the wall [7]. The standard logarithmic relation for velocity near the wall is given by (10):

$$u^+ = \frac{u_t}{u^*} = \frac{1}{k_a} lny^+ + B \tag{10}$$

where u_t is the tangential velocity to the wall at a distance Δy, k_a is the Karman constant and B is a dimensionless constant. The dimensionless distance to the wall y^+ is given by:

$$y^+ = \frac{u*y}{v} \tag{11}$$

where v is the kinematic viscosity of the fluid.The friction velocity is given by (12):

$$u^* = \sqrt{\frac{\tau_w}{\rho}} \tag{12}$$

τ_w is defined as the shear stress on the wall and ρ is the specific mass of the fluid.

2.3 Enhanced Wall Treatment

Enhanced wall treatment is a near-wall modeling method that combines the two-layer model with enhanced wall functions. If the near-wall mesh is fine enough to be able to resolve the laminar sublayer then the enhanced wall treatment will be identical to the standard two-layer zonal model. However, the restriction that the near-wall mesh must be sufficiently fine everywhere might impose too large computational requirement. Then, it is necessary the introduction of a near-wall formulation that can be used with coarse meshes as well as fine meshes in order to reduce computational costs.

2.3.1 Two-Layer Model

In the Two-Layer Model, the viscosity-affected near-wall region is completely resolved all the way to the viscous sublayer. The two-layer approach is an integral part of the enhanced wall treatment and is used to specify both dissipation of the turbulent kinetic energy per unit mass ε and the turbulent viscosity in the near-wall cells. In this approach, the whole domain is subdivided into a viscosity-affected region and a fully-turbulent region. The demarcation of the two regions is determined by a wall-distance-based, turbulent Reynolds number, Re_y defined according with 13:

$$Re_y \equiv \frac{\rho y \sqrt{k}}{\square} \tag{13}$$

where y is a distance between the wall and the cell center in normal direction given by (14):

$$y \equiv \min_{\vec{r}_w \in \Gamma_w} \|\vec{r} - \overrightarrow{r_w}\| \tag{14}$$

where $\vec{r}$is the position vector at field point, $\overrightarrow{r_w}$is the position vector of the wall boundary and Γ_w is theunion of all the wall boundaries involved.The fully-turbulent region is calculated through the turbulence models, such as k-ε model. The viscous sublayer is completely resolved by the one-equation of [8] model described in (15):

$$\mu_{t,twolaye\ r} = \rho C_\mu l_\mu \sqrt{k} \tag{15}$$

where the length scale l_μ is computed from [9] and is described in (16):

$$l_\mu = y C_l^* \left(1 - e^{-Re_y/A_\mu}\right) \tag{16}$$

The two-layer formulation for turbulent viscosity is used as a part of the enhanced wall treatment, in which the two-layer definition is smoothly blended with the high-Reynolds-number μ_t definition from the outer region, as proposed by [10]:

$$\mu_{t,enh} = \lambda_\epsilon \mu_t + (1 - \lambda_\epsilon)\mu_{t,twolayers} \tag{17}$$

where λ_ϵ is a blending function, is defined such that the function is equal to 1 far from walls and is zero very near to walls.

2.3.2 Enhanced Wall Functions

In order to introduce a formulation to be used in coarse mesh it is necessary to have a method that can extend its applicability throughout the near-wall region and thus its layers, such as laminar sublayer, buffer region, and fully-turbulent outer region. Additionally, it is necessary to formulate the law-of-the wall as a single wall law for the entire wall region. [11] proposed blending linear (laminar) and logarithmic (turbulent) laws-of-the-wall for incompressible and timeless flow using a function described in (18):

$$u^+ = e^{\Gamma} u_{lam}^+ + e^{\frac{1}{\Gamma}} u_{turb}^+ \tag{18}$$

where Γ is the blending function and is given by (19):

$$\Gamma = -\frac{0{,}01(y^+)^4}{1+5y^+} \tag{19}$$

The general equation for the derivative $\frac{du^+}{dy^+}$ is given in (20):

$$\frac{du^+}{dy^+} = e^{\Gamma} \frac{du_{lam}^+}{dy^+} + e^{\frac{1}{\Gamma}} \frac{du_{turb}^+}{dy^+} \tag{20}$$

The enhanced wall functions allow the fully turbulent law to be easily modified and extended to include other effects such as pressure gradients or variable properties. This formula also guarantees the correct asymptotic behavior for large and small values of y^+ and good representation of velocity profiles in the cases where y^+ is inside the wall buffer region ($3 < y^+ < 10$).

2.4 Menter-Lechner Wall Treatment

Although the two-layer approach is most used nowadays in industrial simulation, used in the Enhanced Wall Treatment has some drawbacks such as: the Wolfstein equation is not compatible with the ε-equation pressure gradient flows; the model tends to oscillate for a coarse mesh with a y^+, as it switches back and forth between time steps, preventing convergence; and regions with very low values of turbulence kinetic energy might easily have a small turbulent Reynolds number. Therefore, such regions will be treated with a near-wall formulation, though they might be away from the wall.

According with [12] the Menter-Lechner near-wall treatment has been developed as an alternative solution that is not based on the two-layer approach. It uses a new low-Re formulation that is designed to avoid the deficiencies of the already described two-layer approach. The objective of the Menter-Lechner near wall treatment is the use of a y^+insensitive near-wall treatment that predicts independently the wall shear stress, used as a boundary condition to the turbulence models. This treatment should switch gradually from wall functions to a low-Re formulation when the mesh is refined. This also requires a

blending of various quantities between the viscous sublayer and the logarithmic region. The wall shear stress τ_w is calculated according to the (21):

$$\tau_w = \rho u^* u_\tau \tag{21}$$

where the friction velocities u^* and u_τ are blended between the viscous sublayer and the logarithmic region accordingly with (22) and (23):

$$u^* = \left[\left(\frac{\mu U_{tan}}{\Delta y} + 0{,}3\rho k\right)\frac{1}{\rho}\right]^{1/2} \tag{22}$$

$$u_\tau = U_{tan}\left[(u^+_{lam})^{-4} + (u^+_{turb})^{-4}\right]^{1/4} \tag{23}$$

The Menter-Lechner near-wall treatment adds a source term to the transport equation of the turbulence kinetic energy k that includes near-wall effects. The standard k-ε model is modified as shown in the following equations (24), (25) and (26):

$$\frac{\partial(\rho k)}{\partial t} + \frac{\partial(\rho k u_i)}{\partial x_i} - \frac{\partial}{\partial x_j}\left[(\mu + \mu_t)\frac{\partial k}{\partial x_j}\right] = G_k - \rho\varepsilon + S_{near\ -wall} \tag{24}$$

$$\frac{\partial(\rho\varepsilon)}{\partial t} + \frac{\partial(\rho\varepsilon u_i)}{\partial x_i} - \frac{\partial}{\partial x_j}\left[\left(\mu + \frac{\mu_t}{1{,}3}\right)\frac{\partial k}{\partial x_j}\right] = 1{,}44\frac{\varepsilon}{k}G_k - 1{,}92\rho\frac{\varepsilon^2}{k} \tag{25}$$

$$\mu_t = 0{,}09\rho\frac{k^2}{\varepsilon} \tag{26}$$

The source term $S_{near\ -wall}$ added in the transport equation of k is active only in the viscous sublayer and accounts for low-Reynolds number effects. It automatically becomes zero in the logarithmic region.

III. METHODOLOGY

The present work consists in the development of the 2D geometry of a T-junction channel simulating two flows, one parallel to the channel and another transversal to the channel. The geometry of the channel is described in Fig. 3. The dimensions presented here are based on those used by [1] and are related to the width of the entrance of the jet stream δ. The value of δ used in this work is equal to 1 m. For the simulation, only the momentum ratio of $M_R = 2$ was considered. The relationship between the values of δ is present in Fig. 4, originating from the work of [1].The geometry described in Fig. 3 differs from the geometry shown in Fig. 4 in its dimension, where it is analysed here in two dimensions, and in the distance between the inlet of the parallel flow and the inlet of the jet stream and between the junction T and the inlet of the flow jet. In the present work, both distances between the inlets of both flows are 100δ and the channel thickness is 0.12m. Such a gap between the entrances is necessary for the flow to become fully developed.

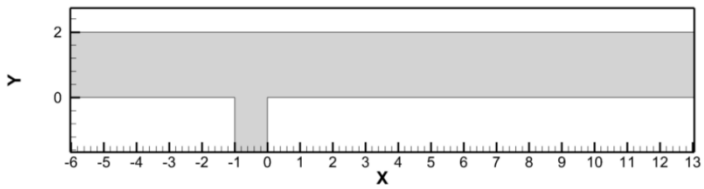

FIGURE 3: GEOMETRY USED IN THE PRESENT WORK.

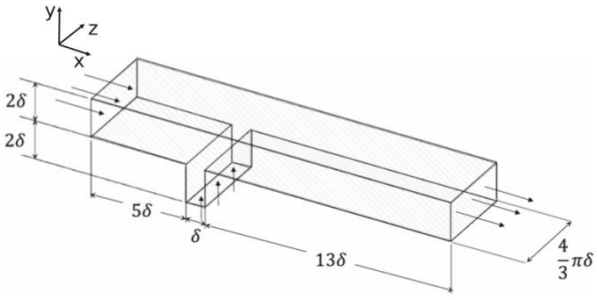

FIGURE 4:3D GEOMETRY USED IN THE WORK OF GEORGIOU E PAPALEXANDRIS (2017).

The present simulation was performed in the ANSYS FLUENT® software, where the flow velocity inlet of the parallel flow is 1 m/s, the outlet pressure of both flows is 0 Pa and kinematic viscosity of the fluid is 0.000111 m² s for all wall functions simulated. The origin point of the simulation is located at the vertex of the jet flow inlet. For the moment ratio $M_R = 2$, the inlet velocity of the jet flow is equal to the inlet velocity of the parallel flow of 1 m/s. The number of Reynolds Re used in this work is 15.000 at the entrance of the parallel flow, the same used in the works of [1]. The domain of the simulation is shown in Fig. 5, where A is the parallel flow inlet, B is the channel walls, C is the jet flow inlet and D is the mixed flow outlet.

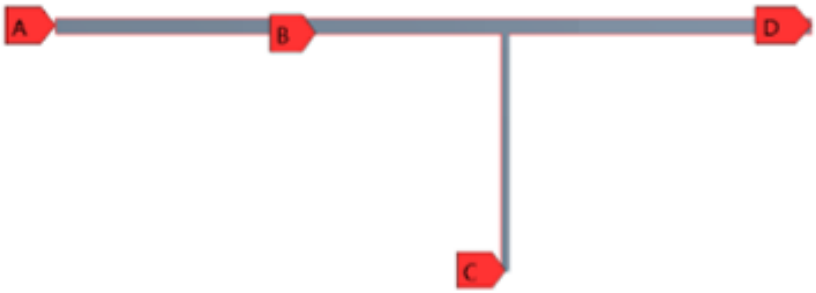

FIGURE 5:DOMAIN OF THE PRESENT SIMULATION

All the simulated cases in the present work use the finite volume method to discretize the governing equations. The interpolation scheme used is QUICK [13] and the SIMPLE scheme was used in pressure and velocity coupling. For the resolution of the system of linear equations the Multigrid technique was used [14]. For the simulation 500.000 iterations were used and was considered converged when all the residues were smaller than 10^{-12}.

The results for 5 different meshes with 200.000, 400.000 and 700.000, 1.000.000 and 1.503.400 elements in each mesh was analysed. Generally, all meshes used in the simulation for all k-ε model can be illustrated according to Fig. 6a and in more detail in Fig. 6b. The meshes present in this study were refined in the regions near the walls and at the vertices of the inlet channel of the jet stream. The selection of such regions was based on the studies of [1],[15], [16], [17] which indicate the appearance of recirculation bubbles at the edges of the jet flow inlet.

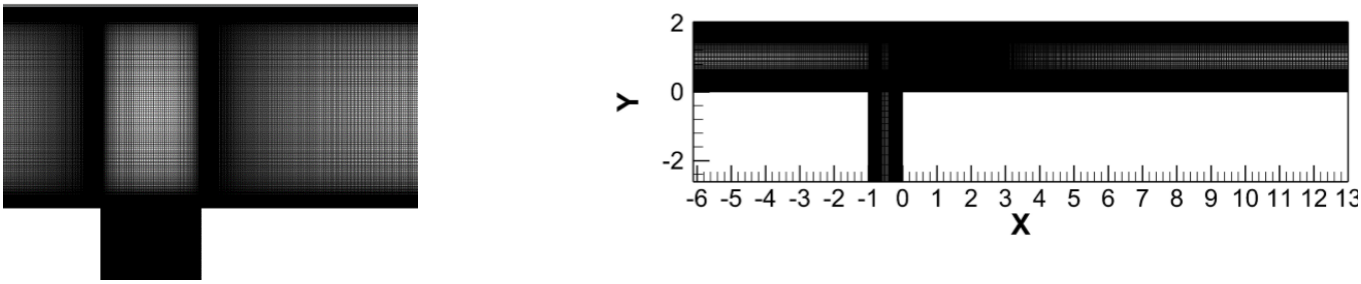

(a) (b)

FIGURE 6: STANDARD MESH USED IN THE SIMULATION OF THE PRESENT WORK.

To analyse the convergence of the result a mesh with 1.503.400 elements were used due to the higher computational precision of the mesh.

IV. RESULTS

The results obtained in the simulations of the present work were calculated through the turbulence model k-ε for different wall functions. The results were compared with the LES simulation performed by [1] using their own software. In this section, important parameters are discussed such as recirculation bubble size, u-velocity vector profile, velocity u^+ profiles, turbulent kinetic energy production and streamlines.

4.1 Streamlines and the recirculation bubble size

The study of the average velocity stream lines is of most importance, since through its analysis, the behaviour of the flows can be identified, for example: mixing zones and layers of separation of the flows. Figure 7 shows the streamlines found in the work of [1] (a) and the those found in k-ε models: Standard Wall Function (b), Enhanced Wall Treatment (c) and Menter-Lechner Wall Treatment (d).Some important characteristics of the flow are described in Fig. 7. According to [1], for the parallel flow, the velocity profile remains unchanged before the jet flow inlet region. However, as the parallel flow approaches the jet flow inlet region, the flow lines of the parallel flow tilt in a vertical direction, since the parallel flow cannot pass through the jet stream. In this way, the parallel flow bypasses the jet stream as an obstacle. The same occurs or the jet flow, as it cannot penetrate the parallel flow it tilts until it is becomes parallel to the channel.

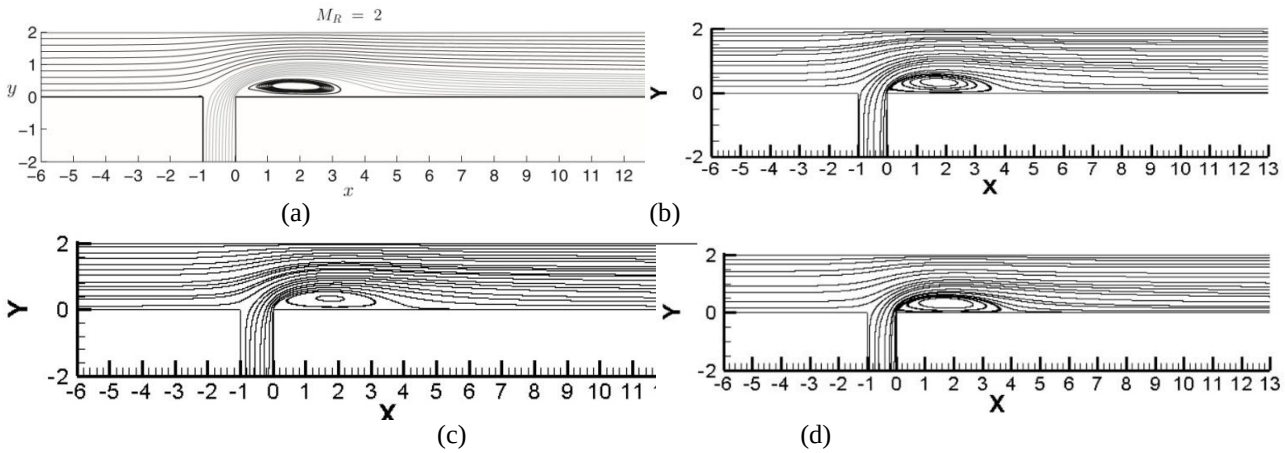

FIGURE 7: STREAMLINES FROM THE WORK OF GEORGIOU E PAPALEXANDRIS (a) AND FROM THE PRESENT WORK (b,c,d).

The slope of the jet stream generates the recirculation bubble downstream of the inlet of the jet stream. The shear layer between the flows can be easily visualized in Fig. 7 (b,c,d). According to Fig. 7 (a), it is possible to ascertain the size of the recirculation bubble in the work of [1] in which the bubble extends to the value of approximately x = 5.

4.2 Contour of the average magnitude velocity

Figure8 shows the contour of the field of magnitude of velocity between the work of [1] and the present simulation.

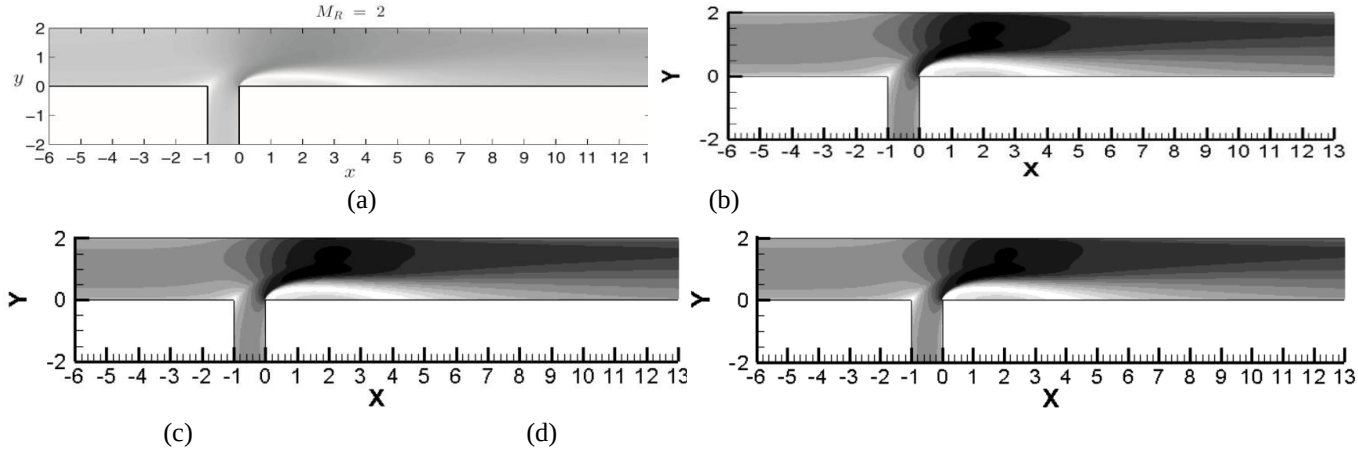

FIGURE 8: CONTOUR OF THE AVERAGE MAGNITUDE VELOCITY FOUND IN THE WORK OF [1] (a) AND K-E MODEL STANDARD WALL FUNCTION (b), K-E MODEL ENHANCED WALL TREATMENT (c), K-E MODEL MENTER-LECHNER WALL TREATMENT (d).

For both results, a second recirculation bubble was found at the vertex upstream of the inlet of the jet stream. The two structures were also found in the results of [18] and [19] and are typical of jets in unconfined parallel flows. In the same work of [20] flow characteristics were found for T-channel. Analysing Fig. 8, the equality in the results can be observed. It is also possible to identify a progressive increase in the magnitude of the velocity from the inlet of the parallel flow once the particles of the parallel flow accelerate while circumventing the jet flow in all results. Such acceleration occurs due to the reduction of the cross-sectional area of the parallel flow due to the Venturi effect. In addition, the jet flow also has a strong acceleration bypassing the parallel flow since the jet flow is limited in the upper part by the parallel flow and in the lower part by the recirculation bubble, reducing the cross-sectional area of the jet stream and increasing its acceleration also through the Venturi effect. It is also possible to notice the occurrence of a second recirculation bubble upstream of the entrance of the jet stream in the channel for all situations analysed. The appearance of the second recirculation bubble can be attributed to the adverse pressure gradient present at the recirculation bubble area, generating the second separation region present in Fig. 8.

4.3 U velocity profile

The profiles of the medium velocity component u (mean velocity U) are described in Fig. 9. The graphics show the comparison between the velocity profile graphs found in the present work, using the stationary k-ε models: Standard Wall Function (b), Enhanced Wall Treatment (c) and Menter-Lechner Wall Treatment (d), and the work of [1], and the transient model LES.

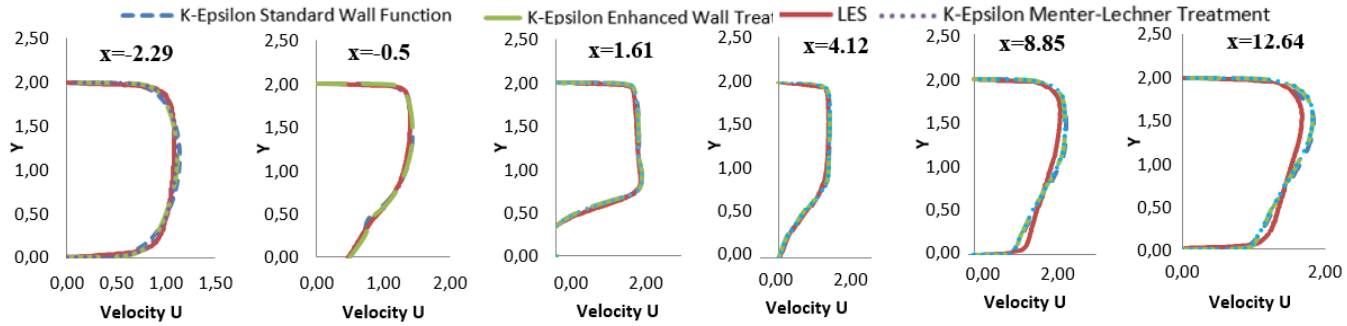

FIGURE 9: COMPARISON OF THE AVERAGE VELOCITY U BETWEEN THE PRESENT WORK AND THE WORK OF [1] FOR DIFFERENT VALUES OF X.

Figure 9 clearly demonstrates the Venturi effect and the increase of velocity of both the parallel and jet streams. For x = -2.29, the region of the parallel flow inlet shows a symmetrical velocity profile, typical of a fully developed flow. When advancing to the inlet region of the jet stream, the symmetry of the velocity profile is lost. At the beginning of the bubble, for x = 1.61, the mean velocity profile is typical of medium velocity profiles containing recirculation bubble. After the recirculation region, the restablishing of the channel flow occurs, however for all the k-ε models, such restablishing occurs more slowly.

4.4 Turbulent Kinetic Energy K Production Profile

The profiles of the turbulent kinetic energy production K are described in Fig. 10. The comparison between the graphs of K production profiles found in the present work, using the stationary k-ε models: Standard Wall Function, Enhanced Wall Treatment and Menter-Lechner Wall Treatment, and the work of [1], and the transient model LES.

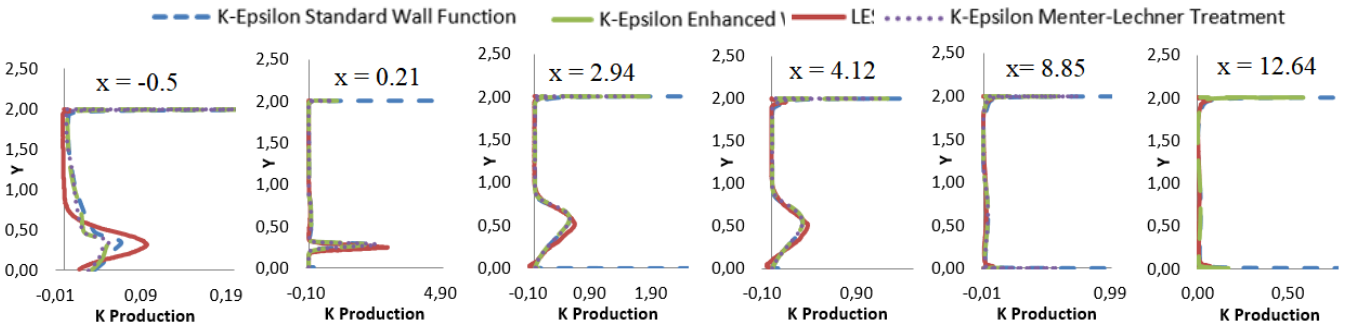

FIGURE 10: COMPARISON OF THE PRODUCTION K BETWEEN THE PRESENT WORK AND THE WORK OF [1] FOR DIFFERENT VALUES OF X.

In addition, the negative K production values found by [1] were not found in the current simulation. However, the higher production values of K coincided with the location of the shear layer between the flows, which leads to conclusion that the production of turbulent kinetic energy comes precisely from the region of the shear layer between the flows. This fact was also found in the study by [1].

4.5 U+ Velocity Profile

Figure 11 shows the comparison between the profiles of u+ at the bottom wall from the present work and the data from the literature at three different streamwise regions: one region upstream the jet and close to the inlet of the crossflow at x = -4,3 and one region downstream the large separation bubble at x = 8,66 and another region further distant from the large separation bubble x = 12,64.According to the results shown in Fig.11 (a), the u^+velocity profile from the k-ε models at x = -

4,3 have a good agreement with the theoretical law of the wall. This is to be expected because at this location, the crossflow remains unaffected by the incoming jet. Additionally, this agreement with the law of the wall indicates the good quality of the results presented by all k-ε models with the exception of the k-ε model standard wall function since its result does not present good agreement with the theoretical law of the wall. The results from all k-ε models at the nearest region downstream the separation bubble in Fig.11 (b), at x = 8.66, deviate considerably from the law of the wall. Specifically, the profiles from the literature and from the k-ε model show an inflection point in the log-law region. This profile behaviour is typical of wall-bounded flows with large separation zones and its occurrence is due to the adverse pressure gradients that are developed downstream those zones as described by [1].There is also can be seen, in Fig.11 (c) that the deviation from the law of the wall exists at the regionx = 12.64, however, this deviation is smaller than at x = 8.66. Such behaviour confirms that further downstream the T-junction and the jet flow inlet, a channel flow will be re-established.

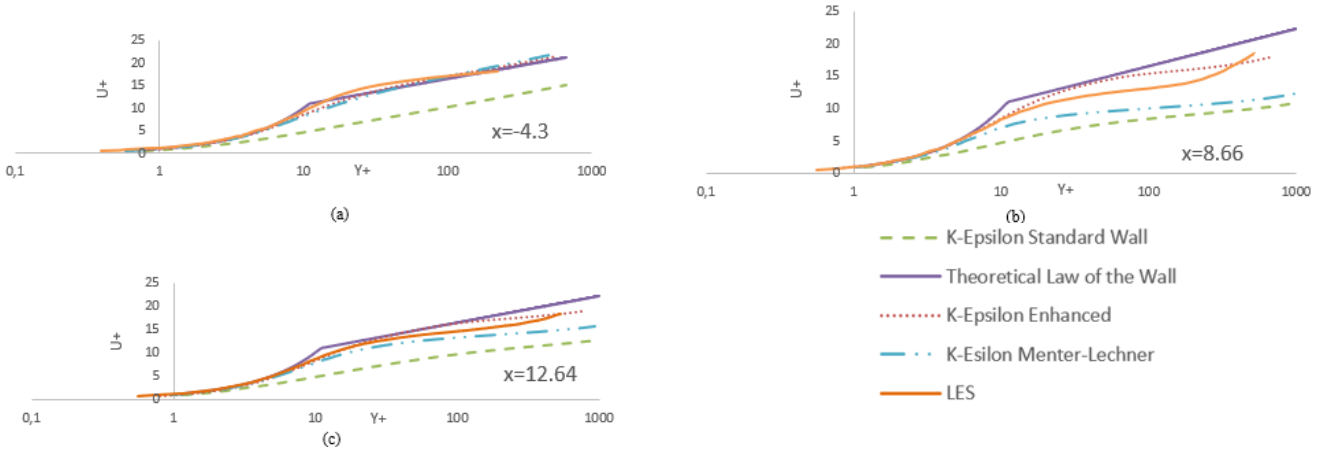

FIGURE 11: COMPARISON U+PROFILES AT THE CHANNEL BOTTOM WALL FROM THE PRESENT WORK AND THE WORK [1] FOR DIFFERENT X VALUES.

Comparing the profiles from each of k-ε turbulence model, the k-ε model Enhanced wall treatment showed best results for all regions, as the k-ε model Menter-Lechner wall treatment displayed larger deviation at x = 8.66. The k-ε model standard wall function diverged significantly from the results obtained by both the other models analysed and by the theoretical curves of the wall law in the turbulent region.

Figure12 shows profiles of u^+at the upper wall and at three different streamwise regions: one region upstream the jet and close to the inlet of the cross flow at x = -4.3 and one region near downstream the jet flow inlet at x = 0.21 and another region further distant from the large separation bubble x = 12.64.

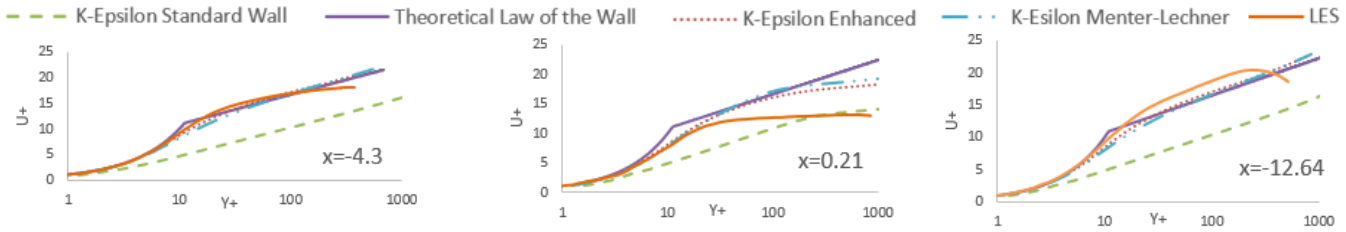

(a) (b) (c)

FIGURE 12: COMPARISON U+ PROFILES AT CHANNEL BOTTOM WALL FROM THE PRESENT WORK AND THE WORK OF [1] FOR DIFFERENT X VALUES.

As in the case of the bottom wall previously described, in Fig.12 (a) at x = -4.30, the top-wall profile follows the theoretical law of the wall. However, at the second region in Fig.12 (b), x =0.21, the deviation from the universal law of the wall is larger. However, u+ maintains a small logarithmic growth. This behaviour can be seen in all models here described, thus in agreement with literature. Such behaviour is attributed to the strong favourable pressure gradient that results from the Venturi effect, that is, the decrease in the cross-sectional area and the ensuing acceleration of the crossflow. Also, as before, in Fig.12 (c) the deviation from the law of the wall that exists at the region x = 12.64 is smaller than at x = 8.66 confirming that further downstream the T-junction and the jet flow inlet, a channel flow will be re-established. Comparing the profiles from each of k-ε turbulence model, the results remain almost the same as for the bottom wall, the k-ε model Enhanced and Menter-

Lechner wall treatment showed best results for all regions. The k-ε model standard wall function diverged significantly from the results obtained by both the other models analysed and by the theoretical curves of the wall law. The results from both walls corroborate to the fact that the turbulence model of two k-ε differential equations with standard wall function does not show good performance in cases with adverse pressure gradient and flow separation, especially in those regions near the wall are regions of great interest.

V. CONCLUSION

In the present work, the turbulence model based on the Average Reynolds Equations (RANS) was used: k-ε model with different wall treatments such as standard wall function, Enhanced Wall Treatment and Menter-Lechner Wall Treatment to analyse the turbulent flow in a T-junction channel having two flows, a flow parallel to the channel and another jet flow, perpendicular to the channel. The results were compared with the studies realised by [1], using the Large Scale Simulation (LES) model. The present work found two recirculation bubbles, one primary bubble downstream of the inlet of the jet stream and another smaller secondary bubble upstream of the jet stream. The same results were found by [1].

The results from all turbulence models are mostly in agreement with the data found by [1], however the k-ε model standard wall functions presented larger deviations for the K production, u^+. The production of turbulent kinetic energy in the wall region was higher in comparison to the result found in the LES simulation for all models. Additionally, the production of turbulent negative kinetic energy was not perceptible, as found by [1]. The k-ε model Enhanced Wall Treatment presented the best results, in accordance with the literature. All models presented smaller length of the recirculation bubble in comparison with literature.

The results presented from the models here analysed indicate that the turbulence model of two k-ε differential equations with standard wall function does not show good performance in cases with adverse pressure gradient and flow separation, especially in those regions near the wall are regions of great interest. Additionally, better results near the wall region were found by the use of k-ε model Enhanced Wall Treatment and Menter-Lechner Wall Treatment.

REFERENCES

[1] M. Georgiou and M. V. Papalexandris . "Numerical study of turbulent flow in a rectangular T-junction". Physics of Fluids APE. (2017).J.ClerkMaxwell, A Treatiseon Electricity and Magnetism,3rded.,vol.2.Oxford:Clarendon,1892,pp.68–73.

[2] Rezende, A.L.T., 2009. Análise numérica da bolha de separação do escoamento turbulento sobre placa plana fina inclinada. Departamento de Engenharia Mecânica, Pontifícia Universidade Católica, Rio de Janeiro.

[3] Jones, W. P.; Launder, B. E. Prediction of laminarization with a two-equation model of turbulence. International Journal of Heat and Mass Transfer. v. 5, p. 31-34, 1972.R.Nicole, "Title of paper with only first word capitalized," J.Name Stand.Abbrev.,inpress.

[4] Launder, B. E.; Sharma, B. I. Application of the energy-dissipation model of turbulence to the calculation of flow near a spinning disk. Letters in Heat and Mass Transfer, v. 1, p. 131-138, 1974

[5] Wilcox, D.C. Reassessment of the Scale-Determining Equation for Advanced Scale Models. AIAA Journal 26(11): 1299-1310, 1988.

[6] Wilcox, D. C. Comparison of two-equation turbulence models for boundary layers with gradient. AIAA journal, v. 31, n. 8, p. 1414–1421, 1993.

[7] Launder, B. E.; Spalding, D. B. The numerical computation of turbulent flows. Computer methods in applied mechanics and engineering, Elsevier, v. 3, n. 2, p. 269–289, 1974.

[8] M. Wolfstein. The Velocity and Temperature Distribution of One-Dimensional Flow with Turbulence Augmentation and Pressure Gradient. Int. J. Heat Mass Transfer, 12:301-318, 1969.

[9] H. C. Chen and V. C. Patel. Near-Wall Turbulence Models for Complex Flows Including Separation. AIAA Journal, 26(6):641-648, 1988.

[10] T. Jongen. Simulation and Modeling of Turbulent Incompressible Flows. PhD thesis, EPF Lausanne, Lausanne, Switzerland, 1992.

[11] B. Kader. Temperature and Concentration Profiles in Fully Turbulent Boundary Layers. Int. J. Heat Mass Transfer, 24(9):1541-1544, 1981.

[12] Inc. ANSYS, "ANSYS Fluent Theory Guide - Release 17.2," 2016. [Online]. Available: https://support.ansys.com/AnsysCustomerPortal/en_us/Knowledge+Resources/Online+Documentation/Previous+Releases/17.2/Fluid+Dynamics/ANSYS+Fluent/Fluent+Theory+Guide?doc_link=/prod_docu/17.2/html/flu_th/flu_th.html..

[13] Leonard, B. P, 1979. A Stable and Accurate Convective Modelling Procedure Based on Quadratic Upstream Interpolation.Computer Methods in Applied Mechanics and Engineering, p. 59-98.

[14] Hutchinson B. R., Raithby G. D, 1986. A Multigrid Method Based on the Additive Correction Strategy. Numerical Heat Transfer, p. 511-537.

[15] Hirota M., Asano H., Nakayama H., Asano T., and Hirayama S., Three Dimensional Structure of Turbulent Flow in Mixing T-junction, JSME Int. J., Ser. B 49, 1070–1077 (2006).

[16] M. Hirota, E. Mohri, H. Asano, and H. Goto, "Experimental study on turbulent mixing process in cross-flow type T-junction," Int. J. Heat Fluid Flow 31, 776–784 (2010).

[17] A. Kuczaj, E. Komen, and M. Loginov, "Large-eddy simulation study of turbulent mixing in a T-junction," Nucl. Eng. Des. 240, 2116 2122 (2010).

[18] S. Muppidi and K. Mahesh, "Study of trajectories of jets in crossflow using direct numerical simulations," J. Fluid Mech. 530, 81–100 (2005).

[19] R. Kelso, T. Lim, and A. Perry, "An experimental study of round jets in cross-flow," J. Fluid Mech. 306, 111–144 (1996).

[20] N. Fukushima, K. Fukagata, N. Kasagi, H. Noguchi, and K. Tanimoto, "Numerical and experimental study on turbulent thermal mixing in aT-junction flow," in The 6th ASME-JSME Thermal Engineering JointConference (American Society of Mechanical Engineers, 2003), pp. 16–20.